Optical Properties of Silica Opal Templates in the Visible and Infrared

Mark Auslender and Shlomo Hava

Department of Electrical and Computer Engineering, Ben-Gurion University, POB 653, Beer-Sheva 84105, Israel

Introduction

Composites of 3D periodic arrays of micro/nanometer scale-size particles have attracted much attention as photonic crystals which may exhibit photonic band gap (PBG) in near infrared (IR) and visible. Among them, artificial silica opals pioneered by two groups [1, 2] are very promising. The opals are formed by a sedimentation process, when SiO_2 spheres are self-assembled in air into FCC lattice [1, 2]. In another approach, a robot aided method to fabricate opal like photonic crystals forcing the FCC structure type was developed [3]. Currently, the opals with a distribution of the sphere's diameter dispersion < 5 % and crystalline order over tens microns, are fabricated [4-8].

Much work was devoted to optical properties of the opals at the wavelengths (λ) below 0.9 μm (the PBG range) including transmission and reflection [4-6], and fluorescence of embedded dye species [5]. Studies on polarized transmission and diffraction [7], and the effective refractive index and group velocity [8] as well have been reported. However, no attention was paid to optical properties of the synthetic opals in IR range. The present work aims at filling this gap. In addition, the visible range is revisited.

Samples and apparatus

For our study we used two wafer templates, of size 1.8 × 2.5 × 0.2 cm^3 and with twice smaller surface area, we assign S1 and S2, respectively, supplied by Opalon – Advanced Materials Co., St. Petersburg, Russia. The Opalon synthesis ensures highly controlled formation of an FCC lattice of mono-disperse SiO_2 spheres with diameters in the range 200 – 600 nm. The long-range crystalline order extension volume is 0.1 mm^3, where the spheres size variation is 3%. Typical SEM images of the templates are shown in Fig.1. The unprocessed surfaces were found to be close the (111) orientation as seen in Fig.1 (a). Farther view reveals a short-range terrace superstructure of unfinished crystal planes.

For the spectral measurements, we used a Bruker Vector-22 FTIR spectrometer in the range 2.5 to 25 μm with the resolution down to 1 cm^{-1}. For the 0.3 – 3 μm range, a Varian Cary 500 UV-VIS-NIR spectrophotometer was employed. Transmission was measured at incidence angles (θ_{inc}) from 0 to 20° with a homemade sample holder, and reflection using a high-precision Bruker grazing-angle unit that allow for varying θ_{inc} and reflection angle (θ_{ref}) from 13° to 80°.

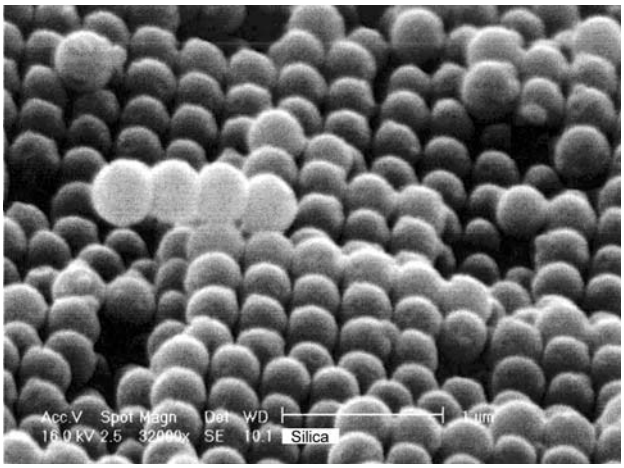

Figure 1: A SEM image (× 3200) of the S1 template.

Results

The normal-incidence transmittance (*T*) spectrum is shown in Fig.2. The agreement between data obtained using the different spectrometers, is noteworthy. The change of *T* with θ_{inc} in the studied range is negligible. Below 0.8 μm, *T* from S1 and S2 differ, see the inset of Fig.2, but above 1 μm, it is nearly the same for both samples. The spectrum shows three stop bands: (i) 0.3 – 0.8 μm (shown at $\lambda \geq 0.5$ μm, see the details in the inset of Fig.2), (ii) 2.7 – 3.6 μm and (iii) 4.8 – 25 μm (shown to 5.5 μm). In the band (i), upon decreasing λ to a cutoff wavelength (λ_G), *T* drops to the apparatus' zero ~ 10^{-10} and does not reenter to any appreciable level down to 0.3 μm. In the bands (ii) and (iii), *T* is less than 0.5 % and 0.2 %, respectively.

The specular and diffused reflection (*R*) spectra were measured at $20° \leq \theta_{inc} \leq 60°$ with step of 5°; see Fig.3. For every θ_{inc}, the scattered *R* was measured at various θ_{ref} in the range $\theta_{inc} \pm \delta$ and typically drops to zero at $\delta \geq 15°$. The spectra show two peak-like bands around ~ 9.0 and ~ 20.9 μm. At $\theta_{inc} > 35°$ the weak shoulder below the 9.0 μm peak in the near-normal incidence *R* transforms into a secondary peak, see Fig.3. Note that the less intense scattered *R* replicates the specular counterpart, as seen in the inset of Fig.3.

Discussion and conclusion

Obviously, the stop band (i) is due to the PBG effect. In the silica opals PBG is directional and is largest in the [111] direction. Hence, our data is compatible with the (111) surface orientation. It was shown [4-6] that λ_G linearly scales with the average sphere's diameter (*a*). We obtained $\lambda_G \approx 582$ nm in S1 and 725 nm in S2, see inset of Fig.2, which yields $a_{S2}/a_{S1} \approx 1.25$. No re-entrance to high transmission, contrary to the case of ultrathin slabs [4-8], may be due to large thickness of our sample as rapid increase of the PBG width was predicted numerically [8] with increasing the number of artificial crystal planes. To attribute the IR spectra, we simulated *R* and *T* with the Brugeman's effective permittivity for the contacting balls at $\lambda >> a$ [9].

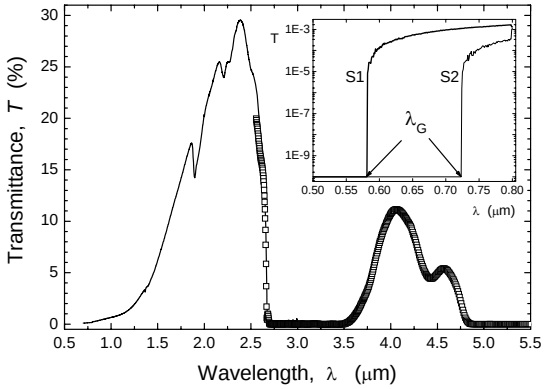

Figure 2: Normal transmission spectrum from the S1; inset – the visible spectrum from the S1 and S2 templates; lines – the Varian Cary 500, squares – the Bruker Vector-22 data.

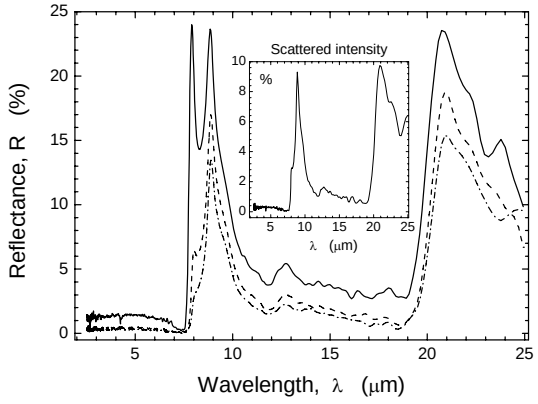

Figure 3: IR reflection from the S1 template at different θ_{inc}; dash-dotted line – 20°, dashed line – 35°, solid line – 50°. Inset – the scattered *R* with $\theta_{inc} = 35°$ and $\theta_{ref} = 45°$.

This analysis easily explained the stop band (iii) and two strong rejection bands in the *R*, seen in Fig.3, by optical properties of SiO_2 – an appreciable extinction at $\lambda > 5$ μm and anomalous dispersion around $\lambda = 9.0$, 20.9 μm [10], respectively, but not the stop band (ii). The calculated and measured position and width of the *R* peak near $\lambda = 9.0$ μm will agree if one assumes the smaller effective refraction index and larger extinction than could be expected from 0.74 fill factor SiO_2 – air mixture. This fact suits well with the porosity of the SiO_2 particles making the opals to be hydrophilic [1, 2]. It is known that in the range 2.7 – 3.6 μm H_2O exhibits absorption which may plausibly explain the stop band (ii).

To conclude, a broad-band transmission and reflection measurements were performed on thick silica opals. The IR transmission exhibited three stop bands, one in the visible and two in the IR range. The IR reflection revealed two strong rejection bands, which are in the anomalous dispersion regions of SiO_2. These results were explained using the PGB concept and effective-medium theory [9] in conjunction with the hydrophilic feature of the silica opals [1, 2].

References

1. V.N. Astratov, et al, Nuovo Cimento D **17** (1995), p. 1349.
2. C. Lopez, et al, Superlattices and Microstructures **22** (1997), p. 399.
3. F. Garcıa-Santamaria, et al, Appl. Phys. Lett. **79** (2001), p. 2309.
4. V.N. Astratov, et al, Phys. Lett. A **222** (1996), p. 349; Yu. A. Vlasov, et al, Phys. Rev. B **55** (1997), p. R13 357.
5. V.N. Bogomolov, et al, Phys. Rev. E **55** (1997), p. 7619.
6. A. Reynolds, et al, Phys. Rev. B **60** (1999), p. 11422.
7. M.V. Rybin, et al, Photonics and Nanostructures **4** (2006), p. 146.
8. J.F. Galisteo-López, et al, Phys. Rev. B **73** (2006), p. 12 5103.
9. D.J. Bergman and D. Stroud, in Solid State Physics (ed. H. Ehrenreich and D. Turnbull, Academic, NY) vol. 46 (1992), p. 148.
10. H.R. Philipp, in Handbook of Optical Constants of Solids (ed. E. Palik, Academic, Orlando) vol. II (1985), p. 757.